2008 American Control Conference
Westin Seattle Hotel, Seattle, Washington, USA
June 11-13, 2008



# Modeling Human Movement with Length-Normalized Action Primitives

Jeffrey N. Shelton
School of Mechanical Engineering
Purdue University
West Lafayette, IN 47907
Email: shelton@purdue.edu

Oh-Sang Kwon
Dept. of Psychological Sciences
Purdue University
West Lafayette, IN 47907
Email: oskwon@purdue.edu

George T.-C. Chiu
School of Mechanical Engineering
Purdue University
West Lafayette, IN 47907
Email: gchiu@purdue.edu

*Abstract*— **Human movement appears constructed of primitives that serve as building blocks for complex motion. Two pioneering descriptions of aimed movement, the *deterministic iterative-corrections* and *stochastic optimized-submovement* models, each assume that such primitives (or submovements) are discrete and non-overlapping. Although these prominent models successfully explain the speed-accuracy tradeoff familiarly known as Fitts' law, they say little about the kinematic shape of submovements. This paper introduces a family of length-normalized action primitives (LNAPs) that produce rigid-body trajectories similar to those seen in human motion, and which agree with Fitts' law. Like the aforementioned models, the LNAP method requires discrete submovements. However, it extends the antecedent models by explicitly bounding potential input profiles. Additionally, it embraces the concept of proportional input noise, a key characteristic of the stochastic optimized-submovement model.**

## I. INTRODUCTION

It has been suggested that complex human motions are constructed from a limited set of movement primitives [1]. This paper proposes a framework for modeling human motion in which movement is driven by a series of energy-balanced profiles, referred to hereafter as *length-normalized action primitives* (LNAPs). Application of LNAPs to a single rigid body produces a dynamic response that agrees with Fitts' Law, is undershooting, and also multiresolutional; these features are characteristic of human movement.

### A. Fitts' Law

Aimed point-to-point movement begins at rest, then travels (roughly) some fixed distance $D$ before stopping inside a target of radius $r$. Such movement is considered to have a relative precision of $(r/D)$. It has been long observed that motions sharing a common relative precision are completed, on average, in an equal amount of time. This is formally known as Fitts' law [2], and may be expressed as

$$t_m = a + b \log_2 \left( \frac{D}{r} \right) \tag{1}$$

where $t_m$ is movement time, and $a$ and $b$ are real constants.

### B. Intermittent Feedback Models

Representations of human motion must deal with the presence of sensory feedback. *Closed-loop* approaches make continuous use of visual and proprioceptive feedback, as seen in optimal feedback control methods [3]. Models that completely ignore such feedback are *open-loop*; included in this group are the minimal jerk [4] and minimal variance [5] theories. Finally, models that incorporate neither open-loop nor closed-loop feedback must instead utilize *intermittent feedback*, assuming that sensory feedback is availed sporadically throughout the movement, but not continuously.

Best-known of the intermittent models are the deterministic iterative-corrections (DIC) model of Crossman and Goodeve [6], and the stochastic optimized-submovement model (SOS) of Meyer et al. [7]. Both models assume that a corrective submovement cannot begin until the prior submovement is completed—an assumption that unfortunately conflicts with evidence of overlapping primitives [8]. Nonetheless, both models have enjoyed considerable prominence in the literature.

According to the DIC model, each submovement travels steadily closer to the target, without overshoot. As long as each submovement produces an exponentially smaller traversal, while consuming an equal period of time, the total movement duration will agree with Fitts' relationship. However, Crossman and Goodeve did place any bounds on the range of input profiles that might work in this manner. Further, they did not consider the effect of neural noise on the command input signal. In an effort to accommodate input noise, the SOS model assumes that submovement variability is linearly related to the submovement's average velocity, thus producing concurrence with Fitts' equation. However, aside from this general description, Meyer et al. do not otherwise constrain the input shape.

In a prior article, the authors demonstrated an intermittent feedback function that agrees with Fitts' law [9]. Expanding on the underlying properties of that function, an entire family of forcing profiles, or LNAPs, is descibed herein. This new methodology utilizes the DIC approach of exponentially smaller traversals to match Fitts' finding, while accommodating the presence of neural noise, as does the SOS model.

### C. Undershooting Behavior

Undershoot is typical in rapid human movement to fixed targets, as individuals increase the amount of undershoot with the level of stochastic disturbance [10]. While some researchers find no bias in aimed movement, it is unusual

978-1-4244-2079-7/08/$25.00 ©2008 AACC.

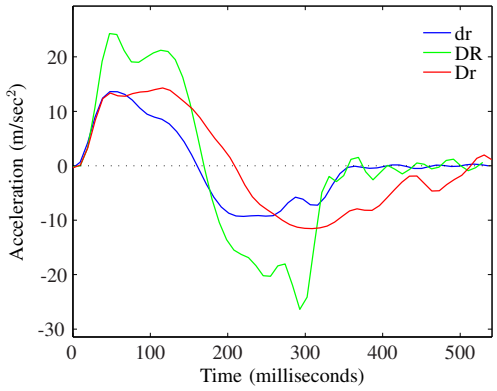


Fig. 1. Average accelerations during 30 trials of forearm rotation by a single subject in three different point-to-point movements. Curves denoted with $D$ traveled twice as far as those denoted by $d$. The target radius $R$ was twice as large as target radius $r$.

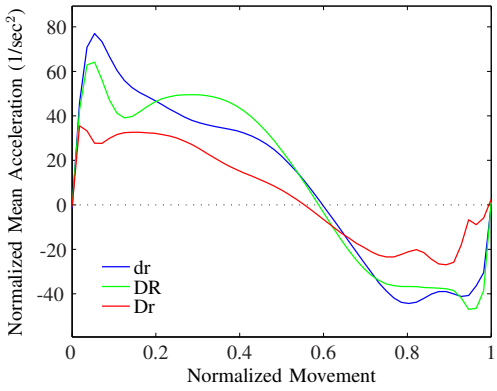


Fig. 2. The same data as in Fig. 1, but normalized by movement length along both axes.

to find a reported overshoot tendency, although overshooting behavior may be evident when attempting to intercept a moving target [11]. Lyons et al. studied vertical point-to-point movement, and showed that undershoot was more likely to occur with downward, rather than upward, movement [12]. This indicates that humans adjust their trajectory to minimize the resultant cost of corrective actions. As detailed below, application of a "noisy" LNAP to a rigid body produces a trajectory that undershoots its target with known probability.

### *D. Multiresolution Nature*

Consider two movements of the same relative precision, but of differing movement distance; these movements are a matched precision pair (MPP). Since they share a common relative precision, the two movements exhibit identical movement durations, as mandated by Fitts' law. However, because they travel differing distances in the same amount of time, their position, velocity and acceleration profiles exhibit unequal amplitudes.

A study by Kwon et al. concludes that humans encode learned hand movement in terms of relative precision, rather than absolute distance [13]. This suggests that movements learned for one relative precision are effectively learned for all other movements sharing the same relative precision. Thus, MPP movements should share more than an identical duration; their trajectories should appear as magnitude-scaled versions of one another [14]. Since an isolated rigid body acts as a linear time-invariant system, it is not surprising that scaling the input (as a function of time) for such as system does, in fact, produce a proportionally scaled output trajectory. This paper proposes that such scaling occurs naturally if input functions are stored as functions of normalized length, rather than time.

As a preliminary look at length-normalized functions, consider the experimental acceleration trajectories of human forearm rotation shown in Fig. 1. Plotted as functions of time, it is somewhat difficult to spot similarities among the curves. When plotted on a length-normalized basis, however, the MPP profiles ('dr' and 'DR') exhibit remarkably similar shapes, as can be seen in Fig. 2. This suggests that motions of a common relative precision can be encoded as a single length-normalized profile, and then scaled to accommodate the desired movement amplitude.

## II. Physical Plant

This paper studies rotation of the human forearm as a proxy for various forms of aimed movement. Using the second-order linear model of van der Helm and Rozendaal [15], the forearm is represented as a rotating rigid link with damping at the pivot; that is,

$$J\ddot{\theta}(t) + B\dot{\theta}(t) = \tau(t) \tag{2}$$

where $\theta$ is the link angle, $J$ is the link polar moment of inertia, $B$ is the rotational damping coefficient, and $\tau(t)$ is the applied torque. Values for $J$ and $B$ are 0.25 kg·m$^2$ and 0.20 kg·m$^2$/s, respectively.

Absent an initial velocity, point-to-point rotation of any mechanical plant in the form of (2) requires that energy be added to the system to induce link rotation. It is assumed that energy is delivered via an applied pivot torque, $\tau$. Once movement is initiated, energy removal may also be required (via negative torque) to halt rotation if energy dissipating processes, such as friction and damping, do not stop rotation inside some desired target interval. As friction is absent in the model of (2), some modicum of negative torque is always necessary to suspend link rotation. This manuscript assumes that energy addition and removal is accomplished via one or more input LNAPs. Thus, the reader may correctly substitute 'torque forcing function' for 'LNAP' throughout the remainder of this manuscript.

## III. Length-Normalized Action Primitives

Unconstrained human motion is generally smooth, displaying a nearly symmetric, bell-shaped, velocity profile. Although imposition of a target does not alter the smoothness characteristic, the velocity profile may be skewed when a spatial constraint is added [16]. Nonetheless, human movement is readily identifiable by a stereotypical kinematic

curve. On the other hand, the proposed LNAP construct allows for a broad range of kinematic responses. So while LNAP constraints are conducive to a "human-like" response, such behavior is not guaranteed. Thus, command signals from the human brain that produce joint torques must be viewed as a subset of the LNAP form. This section introduces four constraints that define a LNAP profile. Common response characteristics are then reviewed.

### A. LNAP Constraints

Regardless of its eventual shape, a LNAP must possess finite energy to avoid driving the system to an infinite position. Further, LNAP activation requires a distinct beginning and end; each LNAP must therefore possess compact support. For convenience, all LNAPs are defined with support over the interval $\zeta = [0\ 1]$, where $\zeta$ is the achieved proportion of desired movement. If the link has rotated halfway to its target, the value of $\zeta$ is 0.5. As a result, any LNAP function, $\psi(\zeta)$, is subject to the following constraint:

*Constraint 1:* Finite Signal Energy with Compact Support

$$\int_{-\infty}^{\infty} |\psi(\zeta)|^2 d\zeta = \int_{0}^{1} |\psi(\zeta)|^2 d\zeta < \infty \qquad \text{(C1)}$$

For a LNAP to accomplish point-to-point movement, it must initially add energy to get the system moving, and then remove energy to decelerate and stop the system. Since work equals force times distance, the mechanical energy injected into the system is equivalent to the area under the $\psi(\zeta)$ curve. If energy dissipating mechanisms are not present, the LNAP must remove all system energy that it has added. This means that the integral of $\psi(\zeta)$ over $\zeta$ must equal zero. Thus, all LNAPs display an oscillatory shape, with both positive and negative intervals. This constraint is expressed as

*Constraint 2:* Mechanical Energy Balance

$$\int_{-\infty}^{\infty} \psi(\zeta) d\zeta = \int_{0}^{1} \psi(\zeta) d\zeta = 0 \qquad \text{(C2)}$$

To exist as a well-defined function of normalized position, a LNAP must map each $\zeta$ in the interval $[0\ 1]$ to a single value of $\psi(\zeta)$. If link rotation stops or reverses direction, then some $\zeta$ exists where both positive and non-positive inputs have been applied, resulting in an ill-defined function. Thus, it must be guaranteed that the system maintains positive velocity throughout the application of any given LNAP. Since the angular velocity of a rotating link reflects its kinetic energy, and no elastic elements are present in the system of (2) to store potential energy, positive velocity is guaranteed by maintaining a positive energy flow as the system moves from $\zeta = 0$ to $\zeta = 1$.

Recall that mechanical energy (work) is equal to applied torque, $\psi(\zeta)$, times distance, $\zeta$. As a result, the area under the LNAP curve between 0 and $\zeta$ represents energy delivered to the system while moving across normalized distance $\zeta$. Assuming that the system starts from rest, it will continue moving forward as long as the area under the LNAP curve remains uniformly positive while $\zeta$ moves between 0 and 1. This restriction on direction change presents a potential problem, given that reversing movements are common in human behavior. However, a study of aimed movement in monkeys indicates that there is always a delay before a movement begins in the opposite direction [17]; this suggests that the brain is processing the initiation of a new primitive. Within the LNAP framework, direction reversal is interpreted as the conclusion of a primitive acting in one direction, followed by the application of another LNAP acting in the opposite direction.

While the need for a positive LNAP integral across the interval from zero to $\zeta \in (0\ 1)$ has been established in the preceding paragraphs, nothing has been mentioned about the forcing function value when $\zeta = 0$. A time-based control input $u(t)$ could feasibly start with zero amplitude, $u(t_0) = 0$, and then begin waiting for the relentless march of time to produce a non-zero input, $u(t_1) \neq 0$, at time $t_1 > t_0$, thereby causing the system to begin moving. However, as a function of normalized position, a LNAP cannot usefully possess a zero initial magnitude. If $\psi(\zeta_0) = 0$, then no torque (force) acts initially on the system, and no movement occurs. As a result, $\zeta$ does not increase, and no non-zero input is ever applied. Thus, to ensure that movement begins in the positive direction, the initial LNAP function value must be positive.

Requiring a jump in $\psi(\zeta)$ at $\zeta = 0$, however, does not imply an infinite power requirement. Incremental work performed by the LNAP across an incremental normalized distance is $dW = \psi(\zeta) d\zeta$. Recalling that power is the time derivative of work, and that Constraint 1 precludes a positional discontinuity (meaning both $\psi(\zeta)$ and $\frac{d\zeta}{dt}$ are finite), the power is bounded; that is, $P = \frac{dW}{dt} = \psi(\zeta)\frac{d\zeta}{dt} < \infty$.

Still, the mere production of muscle force requires some level of energy expenditure; is this another possible infinite power requirement? Since targeted movement allows an individual to prepare for the move, it is presumed that energy is stored in the muscles ahead of the movement, thus alleviating the need for instantaneous energy transfer. We are certainly able to rest a hand on an object at one instant, then push firmly on the object the next instant, as long as we have prepared for the action. In summary, the described need for a positive initial value, along with the requirement for positive area under the LNAP curve, can be written as:

*Constraint 3:* Well-Defined Function with Positive Start

$$\int_{0}^{\zeta} \psi(\zeta) d\zeta > 0, \quad \zeta \in [0\ 1) \qquad \text{(C3)}$$

Although LNAP amplitude is finite (Constraint 1), the function magnitude has not yet been otherwise bounded. As a matter of convenience, mechanical energy added by a LNAP is set to one-half, as is mechanical energy removed by the LNAP. Thus, the absolute integral of mechanical energy (not signal energy) added to, and removed from, the system is set to unity:

*Constraint 4:* Normalized Mechanical Energy

$$\int_{0}^{1} |\psi(\zeta)| d\zeta = 1 \qquad \text{(C4)}$$

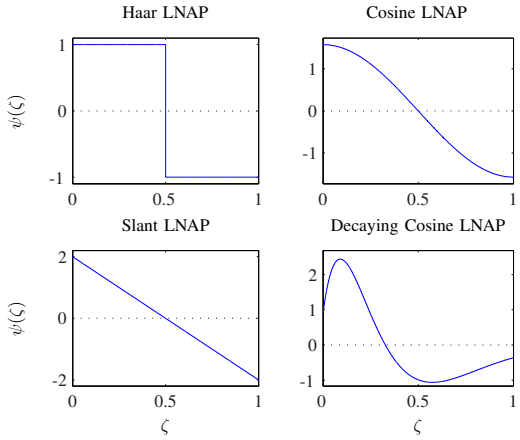


Fig. 3. Possible LNAP Profiles

For the remainder of this paper, the term LNAP refers to a function of normalized position, $\psi(\zeta)$, conforming to constraints C1 through C4. The four profiles displayed in Fig. 3 conform to these restrictions, although an infinite number of alternate LNAP profiles obviously exist.

### B. Undershooting Response

Application of a LNAP input to the system of (2) will produce link rotation. Assume that the link starts at angle $\theta_0$, and the desired endpoint is $\theta_f$. Then the normalized rotation for any angle $\theta$ is

$$\zeta(\theta) = \frac{\theta - \theta_0}{\theta_f - \theta_0} = \frac{\theta - \theta_0}{\alpha} \tag{3}$$

where $\alpha$ represents the desired movement rotation.

Without a loss of generality, assume that the initial angle is zero, and the desired endpoint is unity, so that $\alpha = 1$, and $\zeta = \theta$. If the damping rate, $B$, is zero, then the LNAP will add and remove equal amounts of energy during link movement, resulting in the link rotating precisely to its intended destination, $\theta_f = 1$. When damping is present, however, energy is dissipated. This causes the maximum velocity to be less than that for the non-damped case. Furthermore, the desired endpoint cannot be reached, as the energy balance of Constraint 2 makes no accommodation for energy lost to damping. In fact, if LNAP input is not suspended as the link comes to a stop under the influence of negative torque, rotation will reverse direction. As mentioned in developing Constraint 3, link reversal is an undesired condition. Thus, it is crucial that LNAP application be suspended any time direction reversal is detected.

If damping is present, and all LNAP input is indeed suspended at the instant that rotation comes to a stop, then the link will undershoot its target, just as humans tend to do during targeted movement. The extent of the undershoot can be limited by modifying the LNAP shape, so as to increase the amount of positive energy delivered to the system early in the movement, and thus limiting the amount of energy removed via negative torque until late in the LNAP profile.

### C. Input Disturbance Compensation

Having dealt with the effects of damping, consider next the influence of "noise" on the command signal. Assume that the LNAP input is subject to a white, Gaussian, zero-mean disturbance, $d(t)$, with a variance, $\sigma_d^2$, that is proportional to the square of the command magnitude, such that $\sigma_d^2 = k|\psi(\zeta)|^2$. It has been suggested by Harris and Wolpert [5], [18] that human command signals are corrupted by such input disturbances.

Input disturbances with zero mean will produce end positions that are symmetrically distributed about the target point. Given the human tendency to undershoot a target, it is therefore worth considering what modifications are required to keep a LNAP-driven system from overshooting when proportional input noise is present.

Choose a nominal disturbance bound, $D$, such that

$$D = k_{\text{sd}}\sigma_d \tag{4}$$

where $k_{\text{sd}}$ is a positive real scalar. For a normal distribution, $k_{\text{sd}}$ can be chosen from a standard normal (Z) table to cause D to bound the input disturbance magnitude some desired percentage of the time. For instance, a value of $k_{\text{sd}} = 1.96$ results in the probability of $|d(t)| \leq D$ being 95%.

Substituting (4) into the Harris and Wolpert relationship,

$$\left(\frac{D}{k_{\text{sd}}}\right)^2 = k|\psi(\zeta)|^2$$

After simplifying, a new variable, $\beta$, is introduced to represent the relationship between command magnitude and the disturbance bound:

$$D = k_{\text{sd}}\sqrt{k}|\psi(\zeta)| = \beta|\psi(\zeta)|$$

Given that $k$ is small (experimentally determined to be in the range of k=5 $\times$ $10^{-5}$), $\beta$ likewise has a small magnitude. For reasons discussed below, the range of $\beta$ is restricted to the interval $[0\ \psi(0))$. Since $D$ represents a probabilistic upper bound on $d(t)$, the following relationship is true with a probability consistent with the value of $k_{\text{sd}}$:

$$|d(t)| \leq \beta|\psi(\zeta)|$$

In a worst-case overshoot scenario, the input disturbance acts to increase acceleration under positive torque and hinder deceleration under negative torque. To ensure an undershooting condition, the LNAP can be modified by decreasing the LNAP magnitude by a constant amount across all values of $\psi(\zeta)$. This reduces the energy added to the rotating link, and increases the energy which can be extracted from the system. Although a formal development is not presented here for the sake of brevity, it can be shown that the necessary offset, $\psi_\beta$, to the LNAP is

$$\psi_\beta = \beta$$

To keep the initial value of a LNAP that has been offset in this manner from becoming negative, the value of $\beta$ must be less than the initial value of the unmodified LNAP,

$\psi(0)$. It is for this reason that $\beta$ is bounded above by the initial LNAP amplitude. Within this constraint, however, it is possible to adjust *any* LNAP to undershoot with a desired probability by shifting the LNAP profile downward by a constant $\beta = k_{\text{sd}}\sqrt{k}$. It is also possible to compensate for input disturbances in a non-uniform manner, although the calculations become considerably more complex.

## IV. Scaled LNAPs

In developing the LNAP concept, it has been assumed that all movements have a target endpoint of $\theta = 1$. Movements of differing lengths, however, can also be accommodated using LNAPs. To produce a movement of arbitrary angle $\alpha$, it is possible to "scale" the LNAP function. As defined in (3), normalized movement is

$$\zeta = \frac{\theta - \theta_0}{\alpha}$$

with the value of $\zeta$ ranging from zero at movement initiation ($\theta = \theta_0$) to unity when the desired rotation ($\theta = \theta_0 + \alpha$) is achieved. Assuming, as before, that all movements begin at $\theta = 0$, let

$$\zeta = \frac{\theta}{\alpha} \tag{5}$$

LNAP magnitude is scaled proportionally to match to movement size. Thus,

$$\psi_\alpha(\theta) = \alpha \cdot \psi(\zeta) = \alpha \cdot \psi\left(\frac{\theta}{\alpha}\right) \tag{6}$$

Any offsets or modifications made to the mother LNAP, $\psi(\zeta)$, are thus displayed also in the scaled LNAP, $\psi_\alpha(\zeta)$. When a "noisy" scaled LNAP is applied to the plant of (2), the response is determined by the following equation of motion:

$$J\ddot{\theta}(t) + B\dot{\theta}(t) = \psi_\alpha(\theta(t)) + d(t)$$

On average, the input disturbance, $d(t)$, is zero, so the expected trajectory of the system can be expressed as

$$J\dot{\theta}d\dot{\theta} + B\dot{\theta}^2 dt = \psi_\alpha(\theta)d\theta$$

From (5), it follows that $\dot{\theta} = \alpha\dot{\zeta}$, given a constant movement length, $\alpha$. This relationship, along with the scaled LNAP equivalence of (6), allows the equation of motion to be rewritten without reference to movement angle $\theta$:

$$\alpha^2 J\dot{\zeta}d\dot{\zeta} + \alpha^2 B\dot{\zeta}^2 dt = \alpha^2\psi(\zeta)d\zeta$$

Canceling out the $\alpha^2$ terms, the equation of motion is thus expressed as a function of time, $t$, and normalized movement, $\zeta$, without regard to the desired movement amplitude, $\alpha$:

$$J\dot{\zeta}d\dot{\zeta} + B\dot{\zeta}^2 dt = \psi(\zeta)d\zeta$$

Integrating from an initial state to the state at time $t$, with time-invariant link inertia and damping,

$$\frac{1}{2}J\dot{\zeta}^2 + B\int_0^t \dot{\zeta}^2 dt = \int_0^\zeta \psi(\zeta)d\zeta \tag{7}$$

The first term is normalized kinetic energy. Recalling that linear damper work is $\mathbb{W} = B\int_0^t v^2 dt$, where $v$ is damper velocity, the second term is normalized energy dissipated by the damper. The final term represents area under the LNAP curve, which is normalized energy added to the system by the applied LNAP. Assuming constant values of $J$ and $B$, this relationship holds for all target rotations, $\alpha$. Thus, it is not surprising to discover that all movements governed by (7) reach the same normalized velocity, go the same normalized distance before coming to a stop, and consume the same amount of time.

## V. Discrete LNAPs

If damping is present, the system of (2) will fail to rotate the desired amount under command of a single LNAP. Rather, it will travel forward some fraction of that distance, before damping and negative torque bring the link to a stop. For a time-invariant plant, the rotation fraction, $0 \leq \rho \leq 1$, is the same for all movements conducted using scaled versions of a given LNAP. This can be seen in the energy balance of (7), where energy addition and removal is a function of normalized position, $\zeta$, rather than actual position, $\theta$. If link rotation for a given LNAP stops at $\theta = \rho$ when the commanded rotation is $\alpha = 1$, then link rotation will stop at $\theta = \rho\alpha$ for all other values of $\alpha$ driven by scaled versions of the original LNAP.

Since a single LNAP undershoots its target, it is possible to generate a string of LNAP commands in series, one after another. At the conclusion of each submovement, a new scaled LNAP is created to move the link a target distance $\alpha_{\text{new}} = \theta_f - \theta$. Although each additional submovement will likewise undershoot the target, repeated application of this process can bring the link arbitrarily close to the desired final rotation.

Consider moving a rigid link by means of multiple discrete submovements, with the goal of placing the link inside of a target radius that is no more than angle $r$ away from desired rotation, $D = \theta_f - \theta_0$. This means that total rotation will be in the range $D \pm r$. Subject to constant damping, any rigid link driven by a scaled LNAP, $\psi_\alpha(\zeta)$, will rotate across angle $\rho\alpha$ during a time interval $t_d$. Each time the link stops, a new scaled LNAP is generated and applied. As a result, the total rotation after $N$ submovements becomes

$$\begin{aligned}\Theta &= \rho D + \rho(1-\rho)D + \cdots + \rho(1-\rho)^{N-1}D \\ &= D - D(1-\rho)^N\end{aligned}$$

Since, under LNAP control, the system never overshoots the target rotation, it is sufficient to bound the total movement from below; $\Theta \geq D - r$. As a result,

$$D - D(1-\rho)^N \geq D - r$$

This can be rearranged to show that

$$N = \left\lceil \frac{\log\left(\frac{D}{r}\right)}{-\log(1-\rho)} \right\rceil \tag{8}$$

This indicates that given a sufficient number of submovements, the link can be moved arbitrarily close to the desired rotation, $D$.

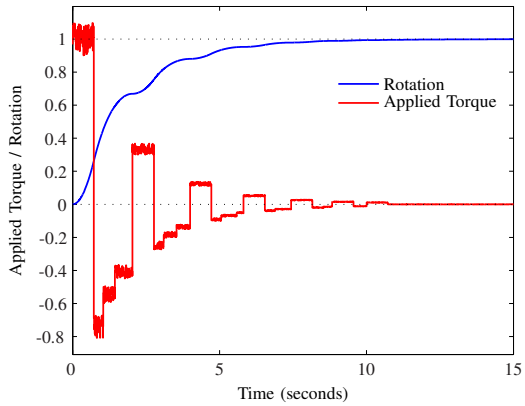


Fig. 4. Application of discrete LNAPs moves the link toward its target without overshoot, despite contamination of the input signal with random noise. From [9].

Let the total time used to generate $N$ scaled LNAPs be $a$. Then the total movement time, $t_m$, consumed in rotating the rigid link utilizing $N$ discrete submovements is

$$t_m = a + N \cdot t_d$$

Approximating $N$ by ignoring the ceiling function from (8),

$$t_m \approx a + \frac{\log\left(\frac{D}{r}\right)}{-\log(1-\rho)} \cdot t_d$$

Noting that $\rho$ and $t_d$ are fixed, define a constant $b$ such that

$$b = \frac{t_d}{-\log(1-\rho)}$$

Then,

$$t_m \approx a + b\log(D/r)$$

This relationship, with the approximation defined as an equality, is Fitts' law. Therefore, repeated application of scaled LNAPs, each based on the same LNAP profile and scaled to reach an unchanging target, produces a response that is consistent with the tradeoff between speed and accuracy laid down by Fitts [2] more than half a century ago.

An example of discrete LNAPs, in this case a "staircase" LNAP that is rescaled and reapplied each time the link comes to a stop, is shown in Fig. 4. Despite noise on the input signal, the link repeatedly undershoots its target, with each successive period of forward movement exponentially smaller in size, but equal in duration. This produces the expected correspondence with Fitts' Law.

## VI. Conclusion

LNAPs provide a framework for studying human movement, with wide latitude given to selecting the shape of any particular LNAP. When applied to a rigid link, these length-normalized forcing functions produce a response that is multiresolutional, undershoots its target, and agrees with Fitts' Law. Future work will demonstrate the stability of discrete LNAPs when moving a rigid body.

## VII. Acknowledgements

The authors would like to thank Dr. Zygmunt Pizlo, of Purdue University, whose theories on the multiresolution nature of movement have inspired much of our research. Sincere appreciation is also extended to an anonymous reviewer who kindly noted technical concerns about a previous version, and suggested additional references; we believe (and hope) this article is improved as a result of that individual's efforts. If not, the blame remains fully ours.

## References

[1] T. Flash and B. Hochner, "Motor primitives in vertebrates and invertebrates," *Current Opinion In Neurobiology*, vol. 15, no. 6, pp. 660–666, Dec. 2005.

[2] P. M. Fitts, "The information capacity of the human motor system in controlling the amplitude of movement." *Journal of Experimental Psychology*, vol. 47, pp. 381–391, 1954.

[3] D. Liu and E. Todorov, "Evidence for the flexible sensorimotor strategies predicted by optimal feedback control," *Journal Of Neuroscience*, vol. 27, no. 35, pp. 9354–9368, Aug. 2007.

[4] T. Flash and N. Hogan, "The coordination of arm movements - an experimentally confirmed mathematical-model," *Journal Of Neuroscience*, vol. 5, no. 7, pp. 1688–1703, 1985.

[5] C. M. Harris and D. M. Wolpert, "Signal-dependent noise determines motor planning," *Nature*, vol. 394, pp. 780–784, 1998.

[6] E. R. F. W. Crossman and P. J. Goodeve, "Feedback-control of hand-movement and fitts law," *Quarterly Journal Of Experimental Psychology Section A-Human Experimental Psychology*, vol. 35A, pp. 251–278, May 1983.

[7] D. E. Meyer, R. A. Abrams, S. Kornblum, C. E. Wright, and J. E. K. Smith, "Optimality in human motor performance: Ideal control of rapid aimed movements," *Psychological Review*, vol. 95, pp. 340–370, Jul 1988.

[8] K. E. Novak, L. E. Miller, and J. C. Houk, "Features of motor performance that drive adaptation in rapid hand movements," *Experimental Brain Research*, vol. 148, no. 3, pp. 388–400, Feb. 2003.

[9] J. Shelton and G. Chiu, "Exponentially segmented positioning of a single link mechanism: A control algorithm that satisfies Fitts' Law," in *Proceedings of the 2007 American Control Conference*, New York City, USA, July 2007.

[10] S. E. Engelbrecht, N. E. Berthier, and L. P. O'Sullivan, "The undershoot bias: Learning to act optimally under uncertainty," *Psychological Science*, vol. 14, no. 3, pp. 257–261, 2003.

[11] D. Lee, N. L. Port, and A. P. Georgopoulos, "Manual interception of moving targets .2. on-line control of overlapping submovements," *Experimental Brain Research*, vol. 116, no. 3, pp. 421–433, Oct. 1997.

[12] J. Lyons, S. Hansen, S. Hurding, and D. Elliott, "Optimizing rapid aiming behaviour: movement kinematics depend on the cost of corrective modifications," *Experimental Brain Research*, vol. 174, no. 1, pp. 95–100, Sep. 2006.

[13] O.-S. Kwon, Z. Pizlo, H. N. Zelaznik, and G. Chiu, "Multi-resolution model of human motor control [abstract]," vol. 6, no. 6, 6 2006, pp. 936–936. [Online]. Available: http://journalofvision.org/6/6/936/

[14] R. A. Schmidt, H. Zelaznik, B. Hawkins, J. S. Frank, and J. T. Quinn, "Motor-output variability: a theory for the accuracy of rapid motor acts." *Psychol Rev*, vol. 47, no. 5, pp. 415–451, September 1979.

[15] F. C. van der Helm and L. A. Rozendaal, *Biomechanics and Neural Control of Posture and Movement*. Springer-Verlang, 2000, ch. Musculoskeletal Systems with Intrinsic and Proprioceptive Feedback, pp. 164 – 176.

[16] K. E. Novak, L. E. Miller, and J. C. Houk, "The use of overlapping submovements in the control of rapid hand movements," *Experimental Brain Research*, vol. 144, no. 3, pp. 351–364, Jun. 2002.

[17] A. Fishbach, S. A. Roy, C. Bastianen, L. E. Miller, and J. C. Houk, "Kinematic properties of on-line error corrections in the monkey," *Experimental Brain Research*, vol. 164, no. 4, pp. 442–457, Aug. 2005.

[18] C. Harris and D. Wolpert, "The main sequence of saccades optimizes speed-accuracy trade-off," *Biological Cybernetics*, vol. 95, no. 1, pp. 21–29, Jul. 2006.